Proceedings of the 26th International Conference on
Port and Ocean Engineering under Arctic Conditions
June 14-18, 2021, Moscow, Russia

Effective moduli for flexure of a floating ice cover due to temperature variations through the depth of the ice

Richard McKenna[1], Greg Crocker[2]
[1] R.F. McKenna Associates, Wakefield, QC, Canada
[2] Dept. of Geography and Environmental Studies, Carleton University, Ottawa, ON, Canada

ABSTRACT

When an ice cover is loaded in flexure, the measured effective elastic modulus is significantly less than Young's modulus for ice. This phenomenon can be explained, at least in part, by the viscoelastic properties of the ice, which are influenced by the structure and temperature of the ice. In this paper, a finite element model that captures the viscoelastic properties of the ice is used to provide context for observed ice behaviour. Although the model represents the full three-dimensional characteristics of columnar-grained S2 ice, the numerical solution is applied to plane stress and plane strain cases for a vertical section through the ice cover.

KEY WORDS: floating ice cover; effective modulus; S2 ice; finite element method; viscoelasticity.

INTRODUCTION

The failure of ice in flexure is important in many engineering and scientific applications including ice loads on sloping structures, icebreaking by ships, ice rubbling and ridge-building forces, and ice cover response to waves. In each case, calculations require that a value be specified for Young's modulus of the ice sheet.

In this paper, we apply a two-dimensional viscoelastic finite element model to examine the effects of depth-dependent ice properties on the effective Young's modulus of freshwater S2 (columnar) ice. The elastic, primary creep and secondary creep formulations account for anisotropies due to the transversely isotropic crystal structure of the ice.

IMPORTANCE OF YOUNG'S MODULUS

Young's modulus (E) appears in many ice engineering calculations. In Westergaard's equations for the extreme fibre stress due to a static load, E appears in a $\log_{10}$ term, suggesting a small effect (ISO 19906, 2019). The icebreaking resistance equations of Linqvist (1989) show that resistance due to bending failure of an ice sheet is proportional to $E^{-0.5}$, which would lead to a more significant effect, given that values for E from the literature vary from about 10 GPa to less than 5 GPa (Traetteberg et al., 1975; Gold, 1994; Snyder et al., 2015). The elastic modulus also influences the properties of flexural gravity waves propagating through uniform and broken ice covers (Wadhams, 1986) and the reflection and transmission of wave energy at a floe edge (Squire, 2007). For waves in sea ice, a reduced or effective modulus is often used to account for primary creep (Bennetts and Squire, 2012). As noted by Vaudrey (1977), the elastic

modulus appears frequently in engineering representations and is a significant contributor to ice behaviour.

For level ice interacting with a sloping structure, ISO 19906 (2019) provides a method for estimating the maximum load due to bending failure of the ice. The governing load is due to the second failure or major crack, and numerical analysis indicates that the horizontal load on the structure due to flexural failure is proportional to about $E^{-0.3}$. This means that decreasing E from about 10 GPa to 5 GPa would increase the ice breaking load by about 25 percent. Although bending failure is only one of several contributions to the overall load on the structure, this range can still be significant, especially in cases in which there is little rubble accumulation. To gain some new insight into the effects of varying ice properties with depth, and how that might affect the effective elastic modulus, we apply a two-dimensional viscoelastic finite element model to realistic ice profile properties.

VISCOELASTIC MODEL FOR S2 ICE

Theory

The present viscoelastic formulation follows generally from McKenna et al. (2021), in which the ice deformation involves additive elastic, primary creep and secondary creep contributions. In this paper, the term "primary creep" is used to represent the transient ice response to loading, which is also referred to in the ice literature as delayed elasticity or anelasticity. The term "secondary creep" is used to represent the steady deformation rate under constant loading. In choosing this terminology that avoids mechanistic descriptions, we recognize that these two creep processes act simultaneously during the deformation process. Whereas McKenna et al. (2021) consider only isotropic ice behaviour in the plane of the ice surface, the equations have been generalized here to describe anisotropic behaviour in three dimensions.

The primary creep strain rate vector is adapted from the solution presented by Zhan et al. (1994) as

$$\dot{\boldsymbol{\varepsilon}}_d = (a_T/n)\left\{\left[\sigma_{d\,eq}/\left(D_d\varepsilon_{d\,eq}\right)\right]^{n-1}[1/(\beta D_d)]\boldsymbol{s_d} - \boldsymbol{\varepsilon}_d\right\} \quad (1)$$

Equation (1), which provides an equivalent solution to that of Zhan et al (1994) for the isotropic case, relies on different expressions for the equivalent primary creep stress and strain, as described below. Equation (1) applies only for monotonic loading. The secondary creep strain rate vector is calculated based on Shyam Sunder and Wu (1989) as

$$\dot{\boldsymbol{\varepsilon}}_v = (3/\beta)\,\dot{\varepsilon}_{v0}\left(\sigma_{eq}/\sigma_1\right)^{n-1}\,\boldsymbol{s}/\sigma_1 \quad (2)$$

In Equations (1) and (2), a_T is a constant, n is the creep exponent, $\sigma_{d\,eq}$ is the scalar equivalent stress for primary creep, D_d is the primary creep spring stiffness, $\varepsilon_{d\,eq}$ is the scalar equivalent strain for primary creep, parameter β is defined below, $\boldsymbol{s_d}$ is the deviatoric stress vector for primary creep, $\dot{\varepsilon}_{v0}$ is a creep constant that depends on temperature and ice structure, σ_{eq} is the scalar equivalent stress, σ_1 is a constant and $\boldsymbol{s}$ is the deviatoric stress for secondary creep.

For polycrystalline S2 ice that is transversely isotropic in the plane of the ice surface, with axes x, y (horizontal) and z (vertical), the equivalent stress (for primary or secondary creep) can be expressed

$$\sigma_{eq} = \left[\frac{3}{\beta}\left\{\frac{m_1}{3}\left(\sigma_{xx}-\sigma_{yy}\right)^2 + \frac{m_2}{3}\left(\sigma_{yy}-\sigma_{zz}\right)^2 + \frac{m_2}{3}(\sigma_{zz}-\sigma_{xx})^2 + 2m_5{\sigma_{yz}}^2 + 2m_5{\sigma_{zx}}^2 + 2m_4{\sigma_{xy}}^2\right\}\right]^{1/2} \quad (3)$$

Based on Shyam Sunder and Wu (1989), Equation (3) can also be written in matrix form as

$$\sigma_{eq} = \left[\frac{3}{\beta}\boldsymbol{\sigma}^T \boldsymbol{G}\, \boldsymbol{\sigma}\right]^{1/2} \tag{4}$$

and the deviatoric stress (for primary and secondary creep) can be written as

$$\boldsymbol{s} = \boldsymbol{G}\, \boldsymbol{\sigma} \tag{5}$$

The transformation matrix relating stresses and deviatoric stresses is

$$\boldsymbol{G} = \begin{bmatrix} \frac{m_1+m_2}{3} & \frac{-m_1}{3} & \frac{-m_2}{3} & 0 & 0 & 0 \\ \frac{-m_1}{3} & \frac{m_1+m_2}{3} & \frac{-m_2}{3} & 0 & 0 & 0 \\ \frac{-m_2}{3} & \frac{-m_2}{3} & \frac{2m_2}{3} & 0 & 0 & 0 \\ 0 & 0 & 0 & 2m_5 & 0 & 0 \\ 0 & 0 & 0 & 0 & 2m_5 & 0 \\ 0 & 0 & 0 & 0 & 0 & 2m_4 \end{bmatrix} \tag{6}$$

in which the stress vector has the form $\boldsymbol{\sigma} = \{\sigma_{xx}, \sigma_{yy}, \sigma_{zz}, \sigma_{yz}, \sigma_{xz}, \sigma_{xy}\}^{\mathrm{T}}$. The constants m_1, m_2, m_4 and m_5 are used to represent the anisotropy in the ice by enhancing the various components of the stress vector when calculating equivalent and deviatoric stresses. Enhanced or increased values of particular stress components imply corresponding enhancement of the affected strain rate components. For S2 ice, the normalizing factor in Equations (3) and (4) is $\beta = m_1 + m_2$.

The equivalent strain measure for primary creep presented in Zhan et al. (1994) does not fully apply to loading situations out of the plane of the ice surface, as in the present bending situation. Based on Shyam Sunder and Wu (1989), the equivalent strain in Equation (1) is

$$\varepsilon_{d\,eq} = \left[\frac{\beta}{3}\boldsymbol{\varepsilon_d}^T \boldsymbol{H}\, \boldsymbol{\varepsilon_d}\right]^{1/2} \tag{7}$$

in which the matrix $\boldsymbol{H}$ is calculated from

$$\boldsymbol{G} = \boldsymbol{G}^T \boldsymbol{H}\, \boldsymbol{G} \tag{8}$$

Finite element implementation

The full viscoelastic model is integrated in time using an Euler method and the resulting equations are adapted for plane stress and plane strain conditions. The continuum solution is solved using the finite element technique described in McKenna et al. (2021). Irregularly-shaped 4-node quadrilateral elements are used with nodes located at each corner. The shape function for this isoparametric element varies bilinearly across the element, while integration of stresses and strains over the element is accomplished using a Gaussian quadrature method in which four interior locations within the element are defined for the shape functions.

PARAMETER ESTIMATION

Elastic constants

The elastic constants for S2 ice used in this paper are developed from the single-crystal values measured by Gammon et al. (1983) using Brillouin spectroscopy. To obtain the S2 polycrystal stiffness or compliance matrix, the matrix for a single crystal (with the *c*-axis in the horizontal plane) is averaged over random orientations in the horizontal plane. The transversely isotropic polycrystal elastic constants used in this paper are the average of the Voigt (constant strain for

all crystals) and the Reuss (constant stress for all crystals) assumptions. Details of these calculations can be found in Sinha (1989), Nanthikesan and Shyam Sunder (1984), and Choi (1997).

Creep constants

Shyam Sunder and Wu (1989) assume that primary and secondary creep anisotropy are the same because the two terms are closely tied in their formulation. Zhan et al. (1994) separate the two because of differences in the mechanisms involved. The latter approach is followed in the present paper.

For primary creep, Zhan et al. (1994) estimate the anisotropy parameters to be $m_1 = 1$, $m_2 = 0.2$ and $m_5 = 0$. The other anisotropy parameter, m_4, is uniquely defined by m_1 and m_2. Practically, when solving Equation (1), a small non-zero value for m_5 is necessary to obtain a valid solution.

For the results presented in this paper where loading times are short and stresses are relatively low, secondary creep does not have a significant effect on the response of the ice. Nevertheless, this term is included in the calculations and appropriate values for the anisotropy constants are provided.

Based on experiments of others, Zhan et al. (1994) estimate the secondary creep anisotropy constants for single crystals to be $a_1 = 1$ (assumed as the reference value in the basal plane), $a_2 = 0.3$ (related to axial stresses in the basal plane to axial stress aligned with the c-axis) and $a_5 = 50$ (related to shear stresses perpendicular to basal-plane). When averaged over many single crystals with random *c*-axis orientation in the plane of the ice surface for S2 ice, these translate to $m_1 = 37.5$, $m_2 = 0.65$ and $m_5 = 25.4$ using the procedures of Zhan et al. (1994, with correction) or Choi (1997). Shyam Sunder and Wu (1989) provide ranges of maximum stress values from constant strain rate experiments on sea ice from which anisotropy constants can be estimated. In general, since the test results for sea ice are sufficiently different from those on freshwater ice, it seems reasonable to use the m_1, m_2 and m_5 estimates derived from the single crystal data.

The other parameter values used in the model are $\dot{\varepsilon}_{v0} = 1.76 \times 10^{-7}\text{s}^{-1}$ (at –10°C) $\sigma_1 = 10^6$ Pa, $n = 3$, $D_d = E\,d\,/\,(c_1\,d_1)$, $c_1 = 9$, $d_1 = 0.001$ m and $a_T = 0.00025$ s^{-1} (at –10°C). Another point of note is that the elastic constants (including Young's modulus, E) from Gammon et al. (1983) at the measured temperature of –16°C, and the creep constants $\dot{\varepsilon}_{v0}$ and a_T have been corrected to the ice temperatures at various depths. A grain size of $d = 0.003$ m (3 mm) is assumed for all calculations, which provides a scaling on the primary creep elastic constant, D_d.

Calibration with uniaxial tests

The finite element model for transversely isotropic viscoelastic behaviour was applied to constant load cases with a plane stress condition in the *x*,*y* plane and a compressive load applied in the *y* direction. Conceptually, this would involve S2 ice loaded in the plane of the ice surface, perpendicular to the axis of the columns, with no constraints in either of the other two coordinate directions. With the above formulation and parameters, the anisotropic model approximates the primary creep strain to within 5 percent after 10 s and 10 percent after 100 s when compared to the equation developed by Sinha (1983), which was based on numerous uniaxial experiments with freshwater S2 ice samples at different temperatures, applied loads and grain sizes. No correction has been applied to the above parameter values to compensate for the difference between Equation (1) and Sinha's equation in the results presented below.

EFFECTIVE MODULUS CALCULATIONS

Setup

To illustrate the viscoelastic effect on the effective bending modulus for a floating ice sheet, a 10 m long beam (x-axis), 1 m in thickness (z-axis) and with unit width (y-axis) is considered. The beam is weightless and loaded or displaced vertically downward at the midpoint. The beam is simply supported at both ends and one end is allowed to displace horizontally so that no additional axial stresses are introduced.

While the application of the results is for a floating ice sheet, the water foundation is not considered in these calculations. The intent is to calculate effective moduli for ice load calculations or other applications in which the water foundation is represented explicitly, either by means of hydrostatics or hydrodynamics.

If the ice beam is narrow, the problem is one of plane stress in the x,z plane, in which there is no restraint (zero stresses) in the y direction. If the beam is wide, the problem can be treated as one of plane strain in the x,z plane and non-zero stresses in the y direction can exist because strains are impeded in this direction. Each of these circumstances is addressed below.

Ice conditions

For midwinter conditions and where the snow cover is minimal, the temperature profile through an ice cover is approximately linear. For freshwater ice, the bottom surface of the ice is at approximately the freezing temperature of water, 0°C, and the top surface in this example is assumed to be –20°C. As mentioned above, the grain size of the S2 ice is 0.003 m in the plane of the ice surface.

Finite element setup

The ice beam is modelled using 80 elements in the x direction and 11 elements in the z direction. Each element therefore has a length of 0.25 m (in x) and a thickness of 0.09 m (in z).

All runs were conducted with a time step of 0.01 s and for a total time of 10 s. The total time of 10 s was chosen to represent the approximate duration of an ice interaction with a sloping structure or a wave cycle.

Equivalent modulus in bending

The moment of inertia of a rectangular beam with respect to an axis passing through its centroid is given by

$$I = (b\, h^3)/12 \tag{9}$$

where b is the width of the beam (in the y direction), and h is the thickness of the beam (in the z direction). The deflection, δ, of a simply supported beam of length, L, loaded vertically in the centre with force, P, is

$$\delta = (P\, L^3)/(48\, E\, I) \tag{10}$$

in which the parameter, E, is Young's modulus. Combining Equations (9) and (10), Young's modulus can be calculated for specific beam dimensions, a deflection and a load.

If a constant load situation is considered, the deflection, δ, varies in time when viscoelasticity is represented and correspondingly Young's modulus becomes an effective value that also varies in time. If a constant loading rate is considered, the effective modulus is obtained from the time-varying applied load and calculated displacement at the midpoint of the beam.

If a constant displacement rate is applied at the midpoint of the beam, the effective modulus is estimated from the time-varying applied displacement and calculated reaction force at the

midpoint of the beam.

Results

Because the effective modulus is affected by the loading conditions, three different situations are considered (i) constant load, (ii) constant loading rate and (iii) constant displacement rate. In each case, the loading is applied vertically downward at the midpoint of the beam. The different runs analyzed in this paper are listed in Table 1. The term "ramp" in Table 1 implies that the load or displacement is applied over the analysis time in a linearly increasing manner up to the maximum value. The applied loads and displacement rates in the various finite element runs were chosen to limit maximum horizontal stresses in the beam to approximately 1 MPa, thereby avoiding conditions that would promote microcracking or flexural failure of the ice beam. It is emphasized that the ice behaviour modelled in this paper does not include the effects of microcracking.

Table 1. Summary of finite element test conditions and results for beam bending

Run	Maximum Value Applied Downward at Midpoint	Load Application	Loading Condition	Effective / Elastic Young's Modulus @ 10 s based on F / δ
1	P = 10 kN/m	constant	plane stress	0.71
2	P = 100 kN/m	constant	plane stress	0.71
3	P = 100 kN/m	constant	plane strain	0.75
4	P = 10 kN/m	ramp	plane stress	0.80 (0.63)*
5	P = 100 kN/m	ramp	plane stress	0.80
6	$\delta = 3 \times 10^{-4}$ m	ramp	plane stress	0.80 (0.63)*
7	$\delta = 3 \times 10^{-3}$ m	ramp	plane stress	0.79

* value calculated when the displacement or load is ramped up to the maximum value over a time of 100 s rather than 10 s

With reference to Table 1, constant loads of 10 kN per m width and 100 kN per m width were applied in Runs 1 and 2 for a plane stress condition. The higher load level was run for a plane strain condition in Run 3. For Run 2, the progression of the effective Young's modulus calculated using Equation (8) is shown by the solid line in Figure 1. Ten seconds after initial application of the load, the applied force and the displacement yielded an effective Young's modulus of 6.5 GPa, which is 0.71 times the elastic or actual value. The dashed curves in Figure 1 are effective Young's moduli estimated from the horizontal stresses and strains at the top and bottom surfaces of the beam. The top surface, which is colder, has a significantly higher effective stiffness than the warmer bottom surface. For the same load as in Run 2, the effective Young's modulus at 10 s for Run 3 with a plane strain condition was 0.75 times the elastic value, indicating that the lateral restraint has the effect of stiffening the beam.

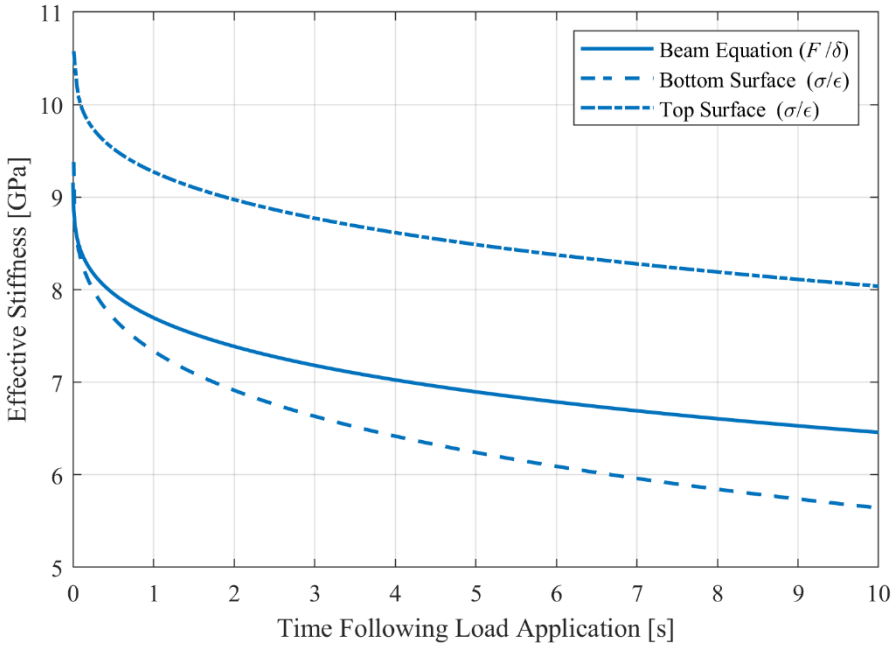

Figure 1. Calculated effective Young's modulus in flexure of a 10 m (long) × 1 m (thick) freshwater S2 ice beam, plane stress condition, top surface temperature –20°C, for a constant applied load of 100 kN/m width (Run 2 in Table 1). An effective composite Young's modulus based on the beam Equation (10) and effective values based on the relationship between horizontal stress and strain at the top and bottom surfaces of the ice are shown.

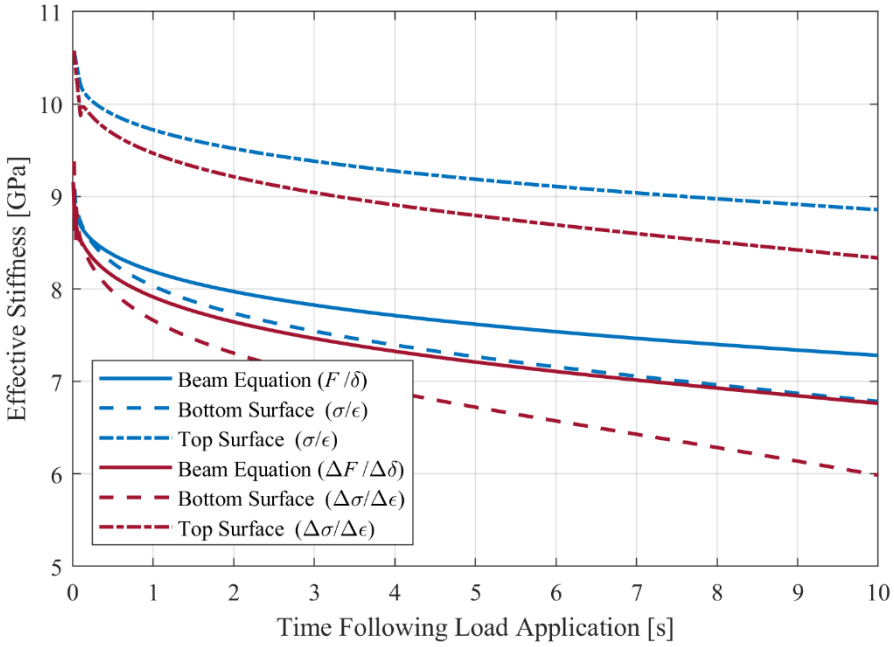

Figure 2. Calculated effective Young's modulus in flexure of a 10 m (long) × 1 m (thick) freshwater S2 ice beam, plane stress condition, top surface temperature –20°C, for a constant loading rate of 10 kN m^{-1} s^{-1} (Run 5 in Table 1). An effective composite Young's modulus based on the beam Equation (10) and effective values based on the relationship between horizontal stress and strain at the top and bottom surfaces of the ice are shown. Also shown are incremental values of the effective Young's modulus.

In Runs 4 and 5, constant loading rates were applied, starting with a zero load and increasing linearly to the same maximum load levels as the constant load tests in Runs 1 and 2. Each of these was run for the plane stress condition. The ratio of effective to actual (elastic) modulus at 10 s is unaffected by the maximum value of the load. The ratio is lower for the constant load than for the ramped load cases, suggesting that the effective modulus is related to the integrated effect of the load rather than just the maximum value. The time series of effective moduli for Run 5 is shown in Figure 2. In addition to the effective values based on accumulated load and displacement, incremental values are also shown. If the particular application under consideration involves instantaneous circumstances, it is worth noting that incremental values of the effective moduli are lower than the accumulated values. Close inspection of Figure 2 shows a slight irregularity in the incremental effective Young's modulus at the top surface of the ice at a time of about 0.1 s. This is due to a slight instability in the solution of Equation (1) under rapidly changing loading – a feature that was not avoided by decreasing the time step.

In Runs 6 and 7, two different constant displacement rates were run for the plane stress condition. For a viscoelastic material, the energy input into the deformation is less when a constant displacement rate is applied than when a constant loading rate is applied. For these constant displacement rate runs, the ratios of effective to actual Young's modulus are essentially the same as for the constant loading rate ones.

DISCUSSION

The results presented in Table 1 and Figures 1 and 2 are based on a model for freshwater S2 ice, with the various components derived from Shyam Sunder and Wu (1989), Zhan et al. (1994) and McKenna et al. (2021). Although the model has been verified for uniaxial loading in the plane of the ice surface, it has not been verified with data for ice beams in flexure.

One important limitation of the model used is that the temperature correction for the creep constants loses applicability at temperatures above about –8°C, e.g. Cole (2020). At these elevated temperatures, which affect the lower half of the ice beam in the above example, the values of the creep constants $\dot{\varepsilon}_{v0}$ and a_T are likely to be greater, leading to lower effective moduli.

In the calculations provided, the primary creep term was based on Zhan et al. (1994) because it is a relatively simple model that captures short-term behaviour for monotonic loading. Equation (1) does not apply for other applications involving non-monotonic loading. McKenna et al. (2021) use a formulation that accounts for loading and unloading situations but its response for loading times in the 10 s range is poor.

Evidence suggests that primary and secondary creep anisotropy for sea ice may not be the same as for freshwater ice. As a result, the anisotropy constants listed in the paper should be used with caution for other than freshwater ice.

It is emphasized that the present model deals exclusively with the effective modulus of the ice material and does not account for the water foundation. Depending on the application, this aspect could be included in the calculation of an effective modulus.

A number of other applications besides beam bending were noted in an early section of the paper describing the importance of Young's modulus. The present model is potentially applicable to a wide variety of such problems and, because the full three-dimensional behaviour is represented in the elastic and creep terms, the finite element model could easily be extended to three dimensions.

CONCLUSIONS

Young's modulus has an effect on the breaking contribution for ice loads on sloping structures. In the example described in this paper, a factor of 10 decrease in Young's modulus results in a 20 percent increase in applied load.

In the beam flexure examples modelled in the paper, the effective Young's modulus decreased to between 71 percent and 80 percent of the elastic values after a loading time of 10 s and to 63 percent after 100 s. Constant loading rate and displacement rates yielded slightly stiffer behaviour than for constant load application. Plane strain, in which the ice beam was constrained laterally in the plane of the ice surface, also increased the effective stiffness of the ice. As a result, lateral restraint is a significant contributor to the effective Young's modulus of ice beams in flexure.

Depending on the application, the above noted difference between elastic and effective values of Young's modulus may or may not be important. As noted in the discussion, creep rates at temperatures above –8°C have been underestimated and appropriate correction would yield decreased effective moduli. For sea ice, we expect the difference between elastic and effective values for Young's modulus to be greater than for freshwater ice because of brine volume effects. To date, we have not addressed the beam flexure problem for sea ice.

The material presented in this paper does not fully represent the model equations, validation cases and basic applications. The intent is to publish full details in the near future and to potentially address the issue for sea ice.

REFERENCES

Bennetts, L. and Squire, V., 2012. On the calculation of an attenuation coefficient for transects of ice-covered ocean, *Proceedings of the Royal Society A: Mathematical, Physical and Engineering Sciences*, Vol. 468, pp. 136-162

Choi, D.H., 1997. *Viscoplasticity and damage mechanics models for rate-dependent materials and their application to ice*, Ph.D. thesis, Department of Civil and Environmental Engineering, Massachusetts Institute of Technology, 202 p.

Cole, D.M., 2020. On the physical basis for the creep of ice: the high temperature regime, *Journal of Glaciology*, Vol. 66, No. 257, pp. 401–414, https://doi.org/10.1017/jog.2020.15

Gammon, P.H., Kiefte, H., Clouter, M.J. and Denner, W.W., 1983. Elastic constants of ice samples by Brillouin spectroscopy, *Journal of Glaciology*, Vol. 29, No. 103, pp. 433-460

Gold, L., 1994. The elastic modulus of columnar-grained fresh-water ice, *Annals of Glaciology*, Vol. 19, pp. 13-18

ISO 19906, 2019. *Petroleum and natural gas industries — Arctic offshore structures*, International Organization for Standardization, 546 p.

Linqvist, G., 1989. A straightforward method for the calculation of ice resistance of ships, *in Proceedings of the 10th International Conference on Port and Ocean Engineering Under Arctic Conditions*, June 12-16 1989, Luleå, Sweden, pp.722-735

McKenna, R., Crocker, G. and Loewen, A., 2021. A finite element model for the deformation of floating ice covers. *Cold Reg. Sci. Technol.*, Vol. 182

Nanthikesan, S. and Shyam Sunder, S. 1994. Anisotropic elasticity of polycrystalline ice Ih, *Cold Reg. Sci. Technol.*, Vol. 22, pp. 149-169

Nanthikesan, S. and Shyam Sunder, S., 1995. Tensile cracks in polycrystalline ice under transient creep: Part II- Numerical simulations, *Mechanics of Materials*, Vol. 21, pp. 281-301

Shyam Sunder, S. and Wu, M.S., 1989. A multiaxial differential model of flow in orthotropic polycrystalline ice. *Cold Reg. Sci. Technol.* Vol. 16, pp. 223–235

Sinha, N.K., 1983. Creep model of ice for monotonically increasing stress, *Cold Reg. Sci. Technol.*, Vol. 8, pp. 25-33

Sinha, N.K., 1989. Elasticity of natural types of polycrystalline ice, *Cold Reg. Sci. Technol.*, Vol. 17, pp. 127-135

Snyder, S., Schulson, E., and Renshaw, C., 2015. The role of damage and recrystallization in the elastic properties of columnar ice, *Journal of Glaciology*, Vol. 61, No. 227, pp. 461-480

Squire, V., 2007. Of ocean waves and sea ice revisited, *Cold Reg. Sci. Technol.*, Vol. 49, pp. 110-133

Traetteberg, A., Gold, L. and Frederking, R., 1975. The strain rate and temperature dependence of Young's modulus of ice, *IAHR Third International Symposium on Ice Problems*, Hanover, New Hampshire, USA, pp. 479-486

Vaudrey, K., 1977. *Ice engineering: study of related properties of floating sea ice sheets and summary of elastic and viscoelastic analyses*, U.S. Naval Facilities Engineering Command, Technical Report R860

Wadhams, P., 1986. The seasonal ice zone, in: *The Geophysics of Sea Ice*, N. Untersteiner [ed], pp. 825-992

Zhan, C., Evgin, E. and Sinha, N.K., 1994. A three dimensional anisotropic constitutive model for ductile behaviour of columnar grained ice, *Cold Reg. Sci. Technol.*, Vol. 22, pp. 269-284